An evaluation of peak and bubble tuning in sub-basalt seismology: modelling and results from OBS data.

ZC Lunnon[1], PAF Christie[2], RS White[1]

[1]*Bullard Laboratories, Cambridge University, Madingley Road, Cambridge CB3 0EZ, UK*

[2]*Schlumberger Cambridge Research, Cambridge CB3 0EL, UK*

Submitted to First Break: 5th August 2003

Published First Break, December 2003, **21**(12), 51-56.

Contact details: E-mail lunnon@esc.cam.ac.uk and pafc1@slb.com

Tel 01223 337173 and 01223 325401

Fax 01223 360779 and 01223 361473

Summary

As part of the iSIMM project (White et al. 2002), a 6,360 in^3 airgun source array was used to acquire, in two passes, a deep seismic profile into a 380 km array of Ocean Bottom Seismometers (OBS) east of the Faroe Islands. The first pass used peak tuning, and the second pass used bubble tuning, with other source parameters constant. The objective was to deliver low frequency energy for deep, long-offset, sub-basalt penetration. The results suggest that towing large guns deep is more important than the tuning method. However, for the gun configuration used, the bubble-tuned data are more compact, less reverberant and easier to pick.

Introduction

The integrated Seismic Imaging and Modelling of Margins (iSIMM) project uses seismic data to characterise extruded and underplated structures at magmatic margins, to constrain the development of new geodynamic models simulating the thermal and structural evolution of such margins. In summer 2002, wide-angle data were acquired by 85 OBS deployed by RRS *Discovery* over two continental margins, one east of Faroes and the second across Hatton Bank. On the Faroes margin (shown in Figure 1), the OBS acquisition was complemented by a 480 km swath acquired by the *Geco Topaz* using three streamers, the longest of which was 12 km. Over the Hatton Bank margin, reflection seismic data were acquired with *Discovery's* 3 km long streamer. The data will be integrated to develop a crustal model from seabed to upper mantle, building on previous work in the area such as FLARE (Fliedner and White 2001). Deep imaging requires return of seismic energy from below the basalt. Several authors (e.g. Mack 1997; Christie et al. *in press*) suggest the use of low frequency bandwidth to overcome the scattering and geometrical losses from rough, high-contrast impedance boundaries associated with stacked lava flows. Enterprise Oil have successfully used low frequency (5-20 Hz) data, recorded by Western Geophysical in imaging the Corrib reservoir beneath shallow basalts offshore Eire, enabling field

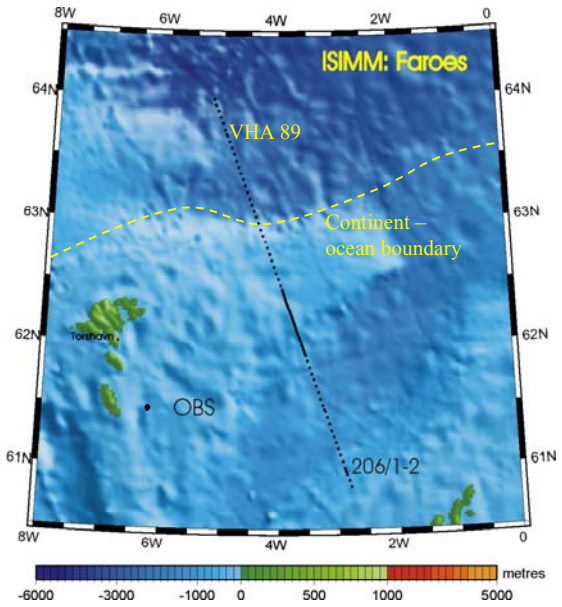

Fig. 1. A map of the profile described in this article, showing the continent – ocean boundary north and east of the Faroes.

development (Dancer et al. 2002). Following discussions with WesternGeco, we designed a source for the Faroes OBS line of large, deep-towed guns and explored the relative benefits of two tuning strategies: synchronising the guns to time-align the primary pulses (peak tuning); and introducing delays to time-align the first bubble (bubble tuning).

Gun depth

From the Rayleigh-Willis relation, the dominant bubble period of a gun signature varies with the cube root of its volume: large guns produce low frequencies. However, the primary followed by the delayed ghost acts as a dipole filter at distances that are far compared to the source depth. This filter has a peak value of two at the frequency for which the source depth is a quarter-wavelength. The downward-travelling, far-field signature has a spectrum with "ghost notch" nulls at 0 Hz and at multiples of frequencies for which the source depth is a half-wavelength. Although depth affects the frequency of maximum ghost enhancement, it is important to note that depth does not affect the octave bandwidth of the ghost-enhanced frequencies: this is 2.32 octaves centred upon the quarter-wavelength frequency (Ziolkowski et al. 2001). A gun is most efficient at its quarter-wavelength depth. The optimum depth for a 1,000 in^3 gun, of which two were used in *Discovery's* source, fired at 140 bar, is approximately 29 m, much deeper than conventionally deployed. However, the deeper a gun, the higher its dominant frequency, as the ambient pressure increases with depth. Figure 2 shows bubble frequency versus depth, estimated from a hydrophone located 1 m from a single 1,000 in^3 gun test-fired during the Faroes survey. Over the 11–23 m depth interval, the trend

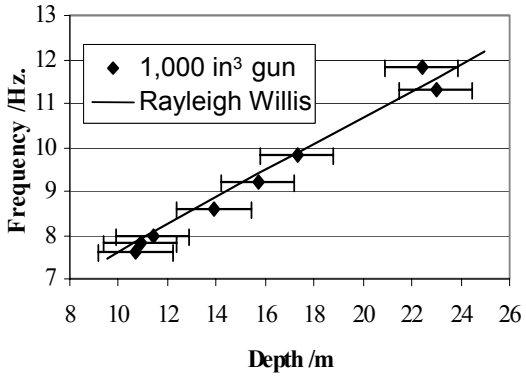

Fig.2. Observed bubble frequency-depth data.

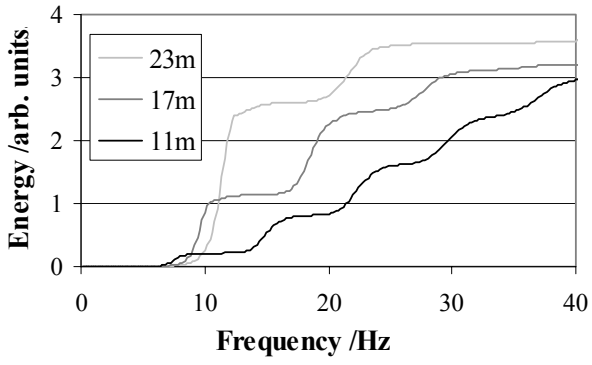

Fig.3. Cumulative energy variation with depth.

follows the Rayleigh-Willis prediction. Figure 3 shows cumulative energy as a function of frequency at three depths from Faroes data. Deeper tow increases gun output, but at the expense of the lowest frequencies. In production, the 1,000 in^3 guns were towed at 16–18 m to produce energy below 10 Hz, and to give good output up to 20 Hz.

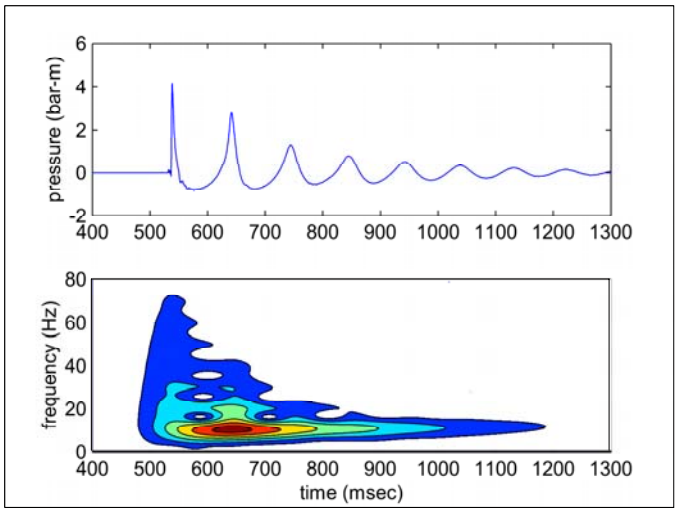

Fig.4. Upper: free-field signature from a single 400 in^3 gun, fired at 10 m depth, with no ghost.

Lower: the frequency-time plot showing that the peak amplitude is about 10 Hz and coincides with the first bubble at about 640 ms. Contour interval 20 dB, arbitrary time origin.

Bubble tuning

A single, free-field signature of a 400 in^3 gun, fired at 10 m depth, is shown in Figure 4, with no ghost. We carried out a time-frequency analysis by windowing the trace with a running Gaussian of half-width 107 ms, and Fourier transforming the trace within each window. The spectral amplitudes are contoured, with the lowest contour at 20 dB, and the highest at 120 dB. The low frequency energy is centred upon the first bubble oscillation.

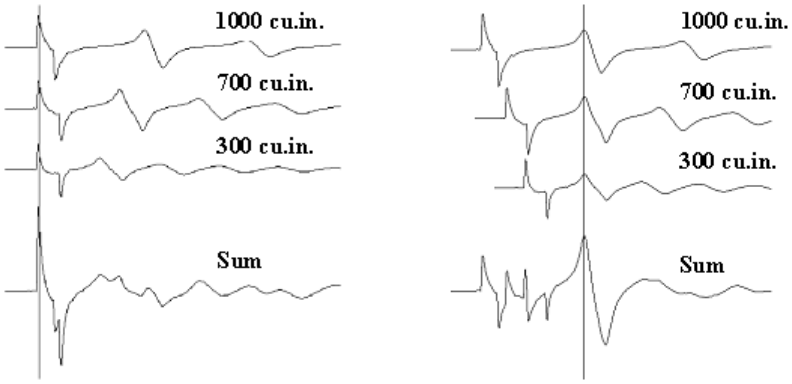

Fig.5. Left: tuning on the peak.

Right: tuning on the bubble.

Conventional peak tuning synchronises the guns so that the first pressure peaks coincide. In bubble tuning, firing delays are applied so that the first bubble oscillations coincide (Figure 5). Peak tuning guns of different sizes minimises the bubble oscillations by destructive interference, but this is not the most efficient use of the available energy. Bubble tuning should be more efficient if low-frequency energy is required. Figure 6 shows pre-survey modelled signatures for both peak and bubble tuning, after filtering through a 20 Hz, low-pass filter simulating earth attenuation. The bubble wavelet has a better peak-to-peak amplitude, is more compact, and should be easier to pick.

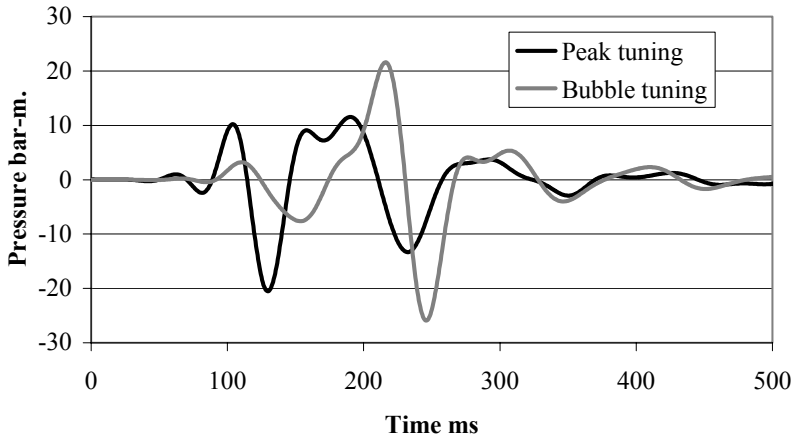

Fig.6. Pre-survey modelled signatures for peak and bubble tuning after the application of a 20 Hz, zero-phase, low pass filter. The bubble-tuned signature is more compact and has a greater peak-to-peak amplitude.

Discovery shot the Faroes OBS line twice, once with peak tuning and later with bubble tuning. All other source parameters were constant. Our bubble-tuning approach differed from that of Avedik (1993) in using Bolt LL guns at a constant depth, instead of GI injector guns at varying depths. Our source comprised four sub-arrays (using 120, 160, 300, 400, 500 and 700 in^3 guns) at a constant 22 m depth, and two 1,000 in^3 guns at depths varying slightly with speed through the water. A photograph of the equipment used is shown in Figure 7. This was the first time variable tuning had been attempted with *Discovery's* acquisition system, and it proved remarkably stable. Timing delays were picked on-board using near-gun hydrophones.

Fig. 7. Two of the beams used (one is barely visible). The closest gun is 700 cubic inches in volume; the beams were deployed over the side using the crane at the top of the picture.

Wavefield reconstruction

Because the near-gun hydrophone system on *Discovery* was insufficient to allow estimation of the far-field signature, we deployed a few Vertical Hydrophone Arrays (VHA) at intervals along the line to monitor the far-field source waveform: see Figure 8. These were intended to measure the direct arrival, but when they were recovered, it was found that the wrong gains had been used, and the water wave was clipped on the peaks. The data from each channel of VHA89 are shown for a near-offset shot in Figure 9. In order to reconstruct the source signatures, up- and down-going wavefield separation was applied. One shot was chosen, and the data from all the live channels (i.e. five traces) were adjusted in time to align the first arrivals. The data were then median filtered. A median filter takes the samples of each trace at time t, ranks them, and takes the middle value. Where there is an even number of traces, the filter takes the mean of the two middle values. This is a robust estimator of the time-aligned, common signal, which is more powerful than stacking and used routinely in VSP processing for wavefield separation. No correction for additional geometrical spreading between top or bottom and middle hydrophones was made, as the difference is 75m/2700m = 2%, which is within the amplitude errors of the sensors. This gave a robust estimate of the clipped downgoing wavefield. The estimated downgoing wavefield was then subtracted from the original traces,

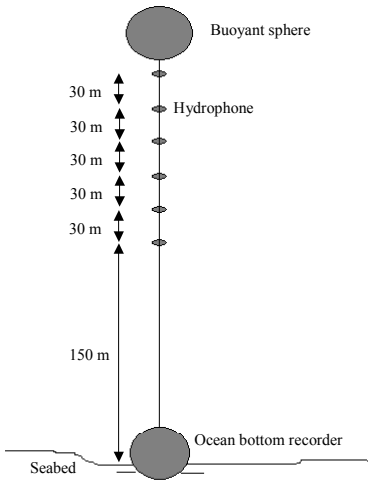

Fig. 8. A schematic diagram of the vertical hydrophone arrays. Each consisted of a heavy ocean bottom recorder, 300m cable, 6 hydrophones and a buoyant sphere deployed as shown.

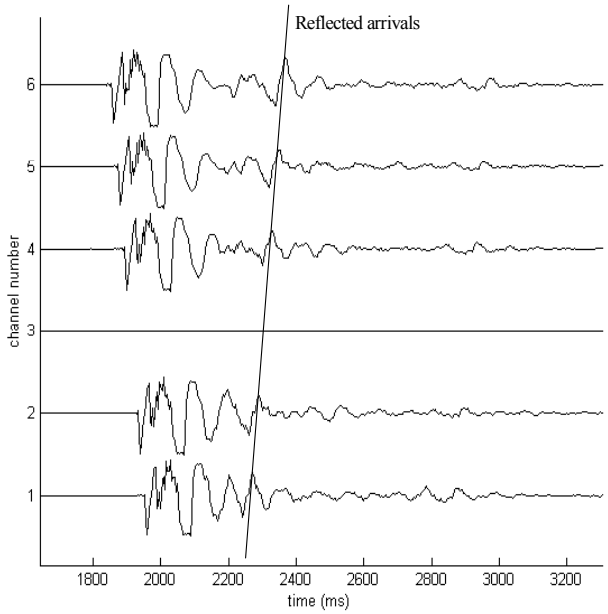

Fig. 9. The initial data used to reconstruct a source waveform. Channel 3 had failed by this point in the survey. The guns are bubble tuned, and the data are taken from VHA89.

leaving a first estimate of the upgoing wavefield. The traces were time adjusted again, such that the upgoing wavefield was aligned. Another median filter was run, in order to remove as much of the residual downgoing wave field as possible. The upgoing and downgoing wavefields were then matched as shown in Figure 10. This shows that although the original downgoing wavefield was clipped due to instrument saturation, a good estimate of the peaks can be found by fitting the upgoing wavefield to it.

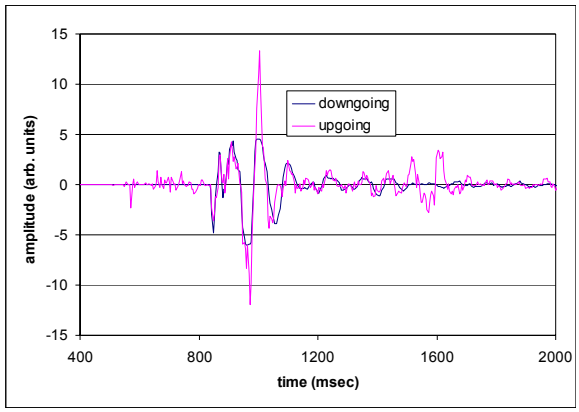

Figure 10: The up- and down-going wavefields from the data in figure 9. The upgoing wavefield has been fitted to the downgoing one.

Comparison with modelling

The source was modelled prior to the survey since library signatures at the volumes or depths required were not available. The measured signals, estimated from VHA 89, are compared with those modelled for both peak and bubble tuning in Figure 11.

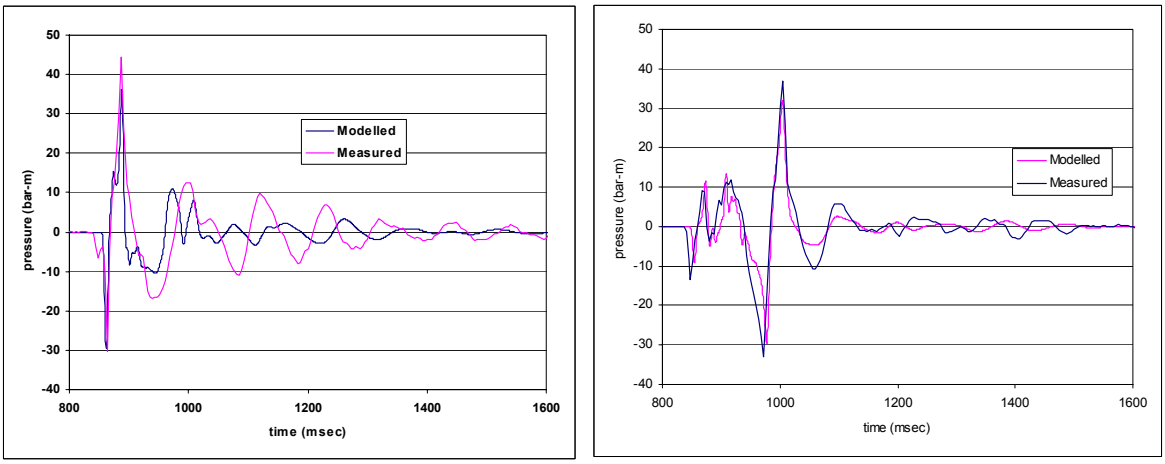

Fig. 11. Modelled and estimated signatures for peak tuning (left) and bubble tuning (right).

The modelling gave some useful pointers to the signatures estimated using the above procedure. The peak-to-peak magnitudes approximately match, although the modelling underestimated the amplitudes found from the signature reconstruction.

	Modelled maximum	Modelled minimum	Estimated maximum	Estimated minimum
Peak-tuned	36.2	-29.5	48.9	-33.5
Bubble-tuned	31.9	-29.5	40.7	-36.3

Table 1: Modelled and estimated far field maxima and minima using the nearest shot to VHA89. All values are in bar-m.

One metric used to analyse how well two signals match is the Normalised Root Mean Square (NRMS). This is defined as:

$$NRMS(\%) = \frac{200 \times \sqrt{\sum_i (S_i - T_i)^2}}{\sqrt{\sum_i S_i^{\,2}} + \sqrt{\sum_i T^2{}_i}} \qquad (1)$$

where S and T are the signals being compared. The magnitude and frequency of the coda when peak tuning were badly predicted, and this is reflected in a NRMS difference of modelled to estimated peak signature of 93%, but the shape of the first peak was reasonably well modelled and the dominant frequency is the same for both the modelled and the estimated signatures. It should be noted that this peak-tuned reverberant coda contributes significant energy to the amplitude spectrum, but impairs resolution and ease of picking. This means that the bubble-tuned signature should show more compact arrivals, and thus be easier to pick. There was a better match between the model and the reconstructed signature for the bubble-tuned array, as demonstrated in an NRMS of modelled to actual bubble signature of 58%, although the details and duration of the precursor were not well matched.

The OBS data

Two vertical geophone profiles from an OBS over oceanic crust at the northern end of the Faroes line are shown in Figure 13, and a photograph of an OBS in Figure 12. Identical processing has been applied: linear moveout at 7 km/s, band-pass filter 5–12 Hz, time-varying gain and range-dependent gain compensation. Both profiles have the same plot gain. Both sections show clear arrivals of similar amplitude and dominant frequency to over 100 km, suggesting that the tuning differences are less important than gun depth and volumes. The bubble-tuned profile is somewhat clearer at the farthest offsets, partly due to lower noise, possibly from different tidal flows. Examining the data after noise reduction shows upper mantle arrivals to 140 km. The bubble tuning shows some other advantages. As suggested by the modelling, its signature is more compact and

Figure 12: An OBS. All the OBS used were four component (three component seismometer and a hydrophone).

easier to pick. It has one main peak rather than two; the ratio between the largest peak and the next largest one is 1.8 on the bubble-tuned data and 1.4 on the peak-tuned data in the 10–30 km range. Tracking the Moho reflection as it emerges through the crustal diving wave is much easier on the bubble-tuned section, which also shows less reverberation at all offsets.

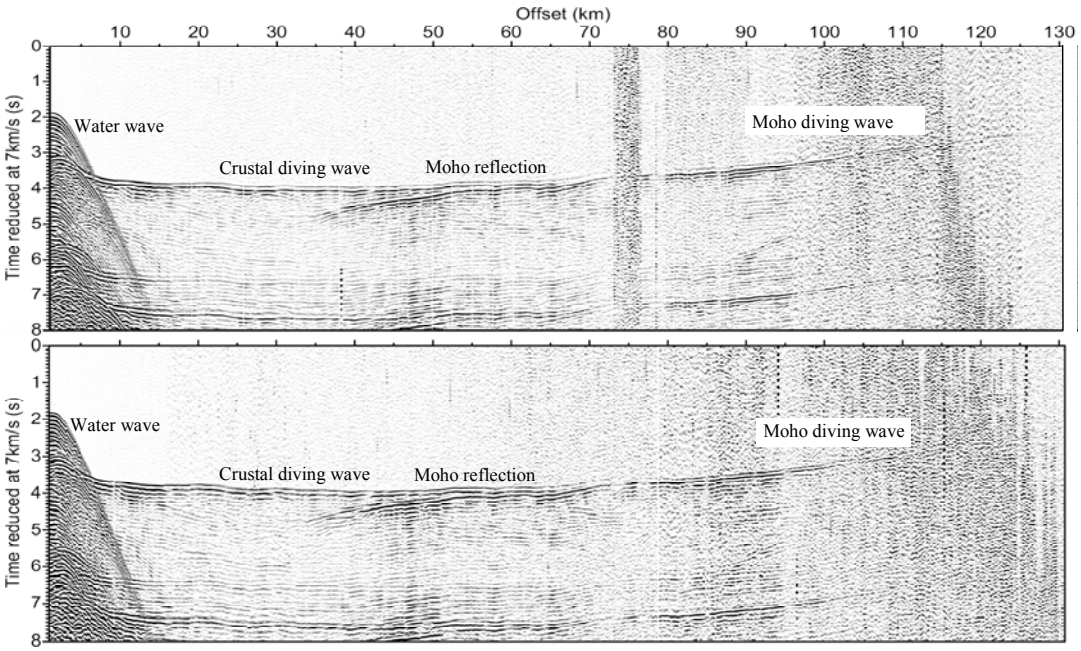

Fig.13. Upper: bubble tuning.

Lower: Peak tuning.

The picked arrivals from the OBS data are being analysed by iSIMM colleagues at Cambridge University to build a deep velocity model to the Moho.

Conclusions

As part of the iSIMM project, we have evaluated peak- and bubble-tuned sources in generating a low-frequency wavelet that penetrates basalt in wide-angle OBS acquisition. Because the ghost operator allows 2.32 octaves of signal enhancement, regardless of source depth, we chose to enhance the low-frequency energy by using large guns, towing them deep and tuning on the first bubble. Pre-survey modelling of the peak- and bubble-tuned arrays showed some benefits for the bubble-tuned array. As expected, we find that the Rayleigh-Willis expression holds for a 1,000 in^3 gun fired at depths in the range 11–23 m. Our data also confirm that increasing source depth trades off improved low-frequency ghost notch response with shorter period bubble oscillation. We were able to estimate far-field signatures using Vertical Hydrophone Arrays, despite the data being clipped. If these are used in the future, the gain setting should be chosen carefully, without over-compensating for the variation in hydrophone sensitivity with depth, and allowing for the possibility that the actual source output might exceed the pre-survey modelled output. The modelled and estimated bubble-tuned signatures match quite well in waveshape, but the estimated peak-to-peak amplitude exceeds the modelled output by about 25%. In the peak-tuned case, the post-peak behaviour

was not well modelled and the output was also under-predicted by 25%. For the OBS survey we used an array of large single Bolt LL guns, with sub-arrays towed at 22 m, and 1,000 in^3 guns towed at 16–18 m. With this modification to Avedik's approach, we found that while both sources gave good results with similar amplitudes and dominant frequencies, the bubble tuning had key benefits over peak tuning: the signal is more compact which makes it easier to pick, shows less reverberation and is more persistent at long offsets. Since OBS data analysis involves mode identification and travel time picking for inverse ray-tracing and subsequent forward modelling, picking quality is a key attribute. Although waveform processing will be attempted on the closely-spaced (2 km) OBS in the centre of the Faroes profile and we will experiment with designature algorithms, designature has not previously been advantageous because of the lack of good shot-to-shot signature estimates and the significant phase changes that take place around the critical offset. This underlines the importance of good signature attributes in the raw data.

Acknowledgements

We thank Peter Sabel, Jon-Fredrik Hopperstad and Andy Harber of WesternGeco for valuable discussions and support during the pre-survey modelling. We also acknowledge the Master and crew of the RRS *Discovery* for their efforts in making the acquisition successful. We thank Alan Roberts for providing the OBS sections and colleagues in the iSIMM team for their assistance and discussions in the data analysis. The iSIMM project is supported by Liverpool and Cambridge Universities, Schlumberger Cambridge Research, Badley Geoscience Limited, WesternGeco, Amerada Hess, Anadarko, BP, ConocoPhillips, ENI UK, Statoil, Shell, the Natural Environment Research Council and the Department of Trade and Industry. However, the views expressed here are those of the authors who are solely responsible for any errors.

References

Avedik, F., Renard, V., Allenou, J.P., Morvan, B., 1993, Single bubble air-gun array for deep exploration. Geophysics **58**, 366–382.

Christe, P.A.F., Gollifer, I., and Cowper, D., Borehole seismic studies of a volcanic succession from the Lopra1/1A borehole in the Faroe Islands, NE Atlantic. Geology of Denmark Survey, in press.

Dancer, P.N., and Pillar, N.W., 2002, Successful sub-basalt imaging with enhanced low frequency 3D seismic data: Corrib Field, West of Ireland, presented at: Frontier Exploration of Volcanic

Continental Margins, Geological Society of London, 17-18 September 2002.*

Fliedner, M.M., and White, R.S., 2001, Sub-basalt imaging in the Faeroe-Shetland Basin with large-offset data. First Break **19,** 247–252.

Mack, H., 1997, Seismic response of Tertiary basalt flows in the northeast Atlantic - a modelling study. 59th Mtg., Eur. Assn. Geosci. Eng., Session: B017.

White, R.S., Christie, P.A.F., Kusznir, N.J., Roberts, A., Hurst, N., Lunnon, Z., Parkin, C.J., Roberts, A.W., Smith, L.K., Spitzer, R., Surendra, A., and Tymms, V., 2002, iSIMM pushes frontiers of marine seismic acquisition. First Break **20**, 782–786.

Ziolkowski, A., Hanssen, P., Gatliff, R., Li, X., and Jakubowicz, H., 2001, The use of low frequencies for sub-basalt imaging. 71st Ann. Internat. Mtg., Soc. Expl. Geophys., 74–77.

* http://www.geolsoc.org.uk/template.cfm?name=abstract_volcanic_dancer